International Journal of Science and Research (IJSR)
ISSN: 2319-7064
SJIF (2022): 7.942

Gradient Different Weight Application In SPECT Volume Estimation

Mohd Akmal Masud[1], Mohd Zamani Ngali[2], Siti Amira Othman[3]

[1, 3]Faculty of Science and Technology, University Tun Hussein Onn Malaysia, Pagoh, Johor, Malaysia
mohdakmalmasud[at]gmail.com

[2]Faculty of Mechanical and Manufacturing Engineering, University Tun Hussein Onn Malaysia, Batu Pahat, Johor, Malaysia
zamani[at]uthm.edu.my

Abstract: ***Single photon emission computed tomography (SPECT) is one of the modalities to detect a cancer lesion and tumour thyroid uptake in nuclear medicine. The low spatial resolution capabilities to form image data of SPECT is quite challenging for the determination required dose for delineation lesion. Robust techniques for automatic or semi-automatic segmentation of objects in sing le photon emission computed tomography (SPECT) are still the subject of development. This paper describes a threshold based which uses the gradient different weight method using the Matlab 2021b algorithm. For every pixel in the grayscale image, the approach calculates the pixel weight. Evaluation is performed based on the NEMA phantom to determine volume, activity concentration, and dice similarity coefficient. In addition, the Monte-Carlo simulated patient data are used to investigate the delineated tumour volumes using the gradient different weight method algorithm.***

Keywords: SPECT, Gradient Different Weight, Intelligent Algorithms

1. Introduction

Iodine-131 (131I) is an essential and widely used radioisotope in thyroid diseases. Single photon emission computed tomography (SPECT) imaging has been considered the most popular method for 131I thyroid uptake radioactive activity quantification. Using the quantitative SPECT/CT method, the accuracy has increased similar to positron emission computed tomography (PET); even the standard uptake value (SUV) used for diagnosis can be obtained. However, due to the complexity to be achieved, quantitative SPECT/CT is rarely applied in clinical practice [1].

The quantification of the lesion and internal organ radioactivity with SPECT has many clinical uses [2]. SPECT imaging offers an accurate three-dimensional (3D) imaging of the radioactivity distribution with attenuation and scatters corrections. Segmentation of these targeted volumes is advantageous for estimating an object's total activity or volume, as in targeted radiation dosimetry and gated cardiac research [3].

Techniques based on threshold [4] and gradient [5] have been employed in dosimetry protocol for radioiodine therapy of differentiated thyroid cancer [6]. Thresholds were determined using a set percentage of the maximum count or statistical techniques such as maximizing interclass variance [7] or multivariate analysis [8]. The fixed percentage threshold is derived directly or related to nearby activity, accurately estimating volume in basic phantom objects. A different strategy for coping with surrounding activity is to adjust the percentage threshold in relation to the level of relative surrounding activity [9].

All segmentation strategies in SPECT are based on the assumption that the volume's activity concentration is homogeneous or close to uniform. The object's non-uniform activity results in an underestimation of its volume [10]. In this case, a reproducible segmentation is achieved, reflecting the volume with a sufficiently steady activity concentration. However, segmentation of an entire item with varied activity may be beneficial in other instances. This article aims to generate the gradient different weight method algorithm with known volume and activity objects. The images are reconstructed using a technique that accounts for both attenuation and scatter [11]. The fractional threshold values that result in accurate segmentation are tabulated under a number of scenarios.

This database is used to establish empirical guidelines for calculating the fractional threshold in any particular case. These criteria are subsequently included in a future image segmentation method. The method employs variable thresholding responsive to ambient activity, object volume and shape, as well as activity concentration uniformity. Additional Monte Carlo simulation tests using Zubal phantom as attenuation maps with a variety of lesion volumes and different activity concentrations are used to evaluate the technique, as well as a comparison to the usage of a NEMA phantom based [12].

2. Method

2.1 Phantom Preparation

The Philips Allegro PET scanner was used to scan the National Electrical Manufacturers Association (NEMA) Inter-national Electrotechnical Commission (IEC) Body Phantom [13]. The NEMA IEC Body phantom is widely recommended for the evaluation of whole-body SPECT imaging. As this phantom had six spherical phantoms with different diameters, we set the 6 volumes of interest (VOI) on the spheres. These spherical phantoms had an inner diameter of 10 mm, 13 mm, 17 mm, 22 mm, 28 mm, and 37

mm, respectively. Therefore, the size of the VOI was set as the inner diameter of the sphere's physical.

212 Mbq131-I will be inserted into a 1000 litre glass bottle for the activity concentration sphere, which is 0.212Mbq/mL. The six spheres with different geometrical will be filled with 0.212Mbq/mL. The initial activity for the first scan of six spheres is 5.22 Mbq, 2.23 Mbq, 1.03 Mbq, 0.51 Mbq, 0.26 Mbq, and 0.11 Mbq for inner sphere diameter 37 mm, 28 mm, 22 mm, 17 mm, 13 mm, and 10 mm, respectively. The weight of the phantom was 12 kg, including the radiopharmaceuticals. The volume and calculating counts were measured using Matlab R2021b software (Mathworks Inc., Sherborn, MA, USA).

The activity of concentration background area is filled with 0.0210 Mbq/mL 131-I based on the NEMA NU 2-2007 standard (NEMA Standards Publication NU 2-2012, 2013). Here, the ratio sphere to background is 10:1, as shown in Figure 1. For the ratio sphere to background 8:1, the activity of concentration background area is filled with 0.0264 Mbq/mL 131-I. Then, the activity concentration in the sphere is the same as the 10:1 ratio. Data were acquired in a three-dimensional (3D) model. The data were reconstructed in a 256×256 matrix with a slice thickness of 9.328 mm, 4.640 mm, and 2.332 mm, respectively. Here, Ordered Subset Expectation Maximization (OSEM) was used to recreate the images. The effective axial field of view was 15.5 cm.

.

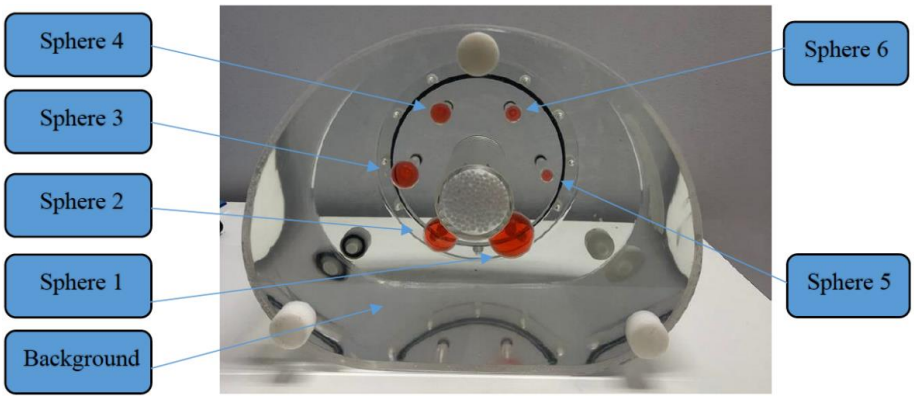

Figure 1: NEMA phantom preparation

2.2 SPECT/CT data acquisition

All acquisition phantom were performed using Philips Brightview XCT with Computed Tomography (CT) capability equipped with a high-energy general-purpose parallel-hole (HEGP) collimator [14]. For each tomographic scan, 40 viewing angles covering 360° and a scatter correction window of 364 keV ±10% were used. Three matrix sizes were tested at 256×256 with pixel sizes of 9.32, 4.64, and 2.33 mm, respectively, as seen in Figure 2.

The phantom was positioned at the centre and close to the detector using the body contouring detection method. The position of collimator setting as vertical -20 cm, longitudinal 73 cm, detector 1 with radius 33 cm, detector 2 with radius 33 cm, as well as step and shoot scan mode set for 40 s/frame. CT scan with the energy of 120 kVp and tube current of 20 mAs was used for attenuation correction as well as to determine the exact location of the subject in the phantom during image processing. The identical SPECT/CT measurements were carried out on the 1st, 2nd, 3rd, and 4th scans with a concentration of 0.212 MBq/mL, 0.097 MBq/mL, 0.058 MBq/mL, and 0.029 MBq/mL, respectively.

Figure 2: Phantom acquisition

2.3 SPECT/CT reconstruction

The acquired SPECT images were reconstructed using JET Stream Brightviewer 2.0, as seen in Figure 3. Iterative reconstruction was performed using 3D orderedsubsets

expectation maximization (OSEM) algorithm [15] that included depth-dependent detector response modelling (resolution recovery), scatter, attenuation correction without post-filtering. The iterations number used is 2 with a fixed subset(s) of 8. The final reconstructed SPECT images consist of matrix sizes 256×256.

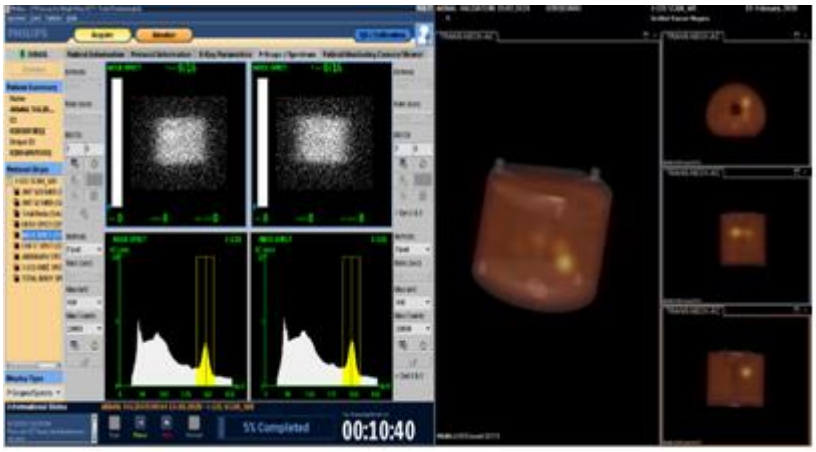

Figure 3: Reconstruction images

2.4 Gradient Different Weight Algorithm

The pixel weight for every pixel in the grayscale image is computed using the gradient difference weight. It is the absolute value of the difference between the intensity of the pixel and the scalar's specific reference grayscale intensity. Pick a reference grayscale intensity value representing the object to be segmented. The weights are returned in the array, having the same size as the input image. The absolute magnitude of the grayscale intensity difference at the pixel position is inversely proportional to the pixel's weight. The weight value is large if the difference is small (thresh value). On the other hand, if the difference is large (thresh value), the weight value is small.

Here is the algorithm of gradient different weight:

```
seedR= 140; seedC = 150; seedP=84;
W = graydiffweight(spect, seed, seedR, seedP ,
'GrayDifferenceCutoff', 1000000000);
thresh =0.1
[BW, D] = imsegfmm(W, seedC, seedR, seedP, thresh);
T = regionprops('table', BW,'Area','Centroid')
```

Remark: The values in this algorithm is just for illustration purpose

Here, seedR represents the row location for pixels with maximum counts in the sphere, seedC represents the column location for pixels with maximum counts in the sphere, and seedP is the frame for the image. Thresh value will be changed until the actual volume of the sphere is obtained.

Through this algorithm, GrayDifferentCutoff should be the pixel value on the boundary targeted volume to be segmented, as shown in the diagram below. However, it is very difficult to determine the value of GrayDifferentCutOff for the gray scale image for the SPECT image, as seen in Figure 4, because the boundary value difference is almost the same as the background. After all, SPECT is a modality that produces a low-resolution image.

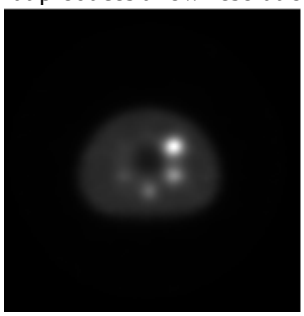

87	86	84	83	81	79
88	87	85	84	82	80
89	88	86	87	86	83
90	90	89	86	86	84
90	90	90	87	88	85
91	91	90	89	88	86

Figure 4: Pixel counts in grayscale image

This study used a phantom NEMA having six spheres to obtain the thresh value equation. Background to sphere ratios of 10: 1 and 8: 1 were conducted to obtain thresh factor values as in Table 1 below.

Table 1: Thresh value calibration

Background Ratio	Ratio Factor	Thresh Value
10: 1	0.004478	5.52
	0.001437	3.2
	0.000326	2.07
	0.000092	1.57
8: 1	0.003685	4.68
	0.000553	2.45
	0.000219	1.85
	0.00004480	1.4

To obtain the value of the ratio factor, the formula below has been used.

Ratio factor, RF = C_{max} / C_{mean} ,

where Cmax is the maximum counts in the sphere and Cmean is the mean counts for the background. After obtaining the thresh value for each appropriate volume, the graph below is plotted. Then, an equation $y = 0.0001x^2$ +

0.0003x - 0.0007, where y represents the ratio factor and x represents the thresh value, as in the Figure 5 below.

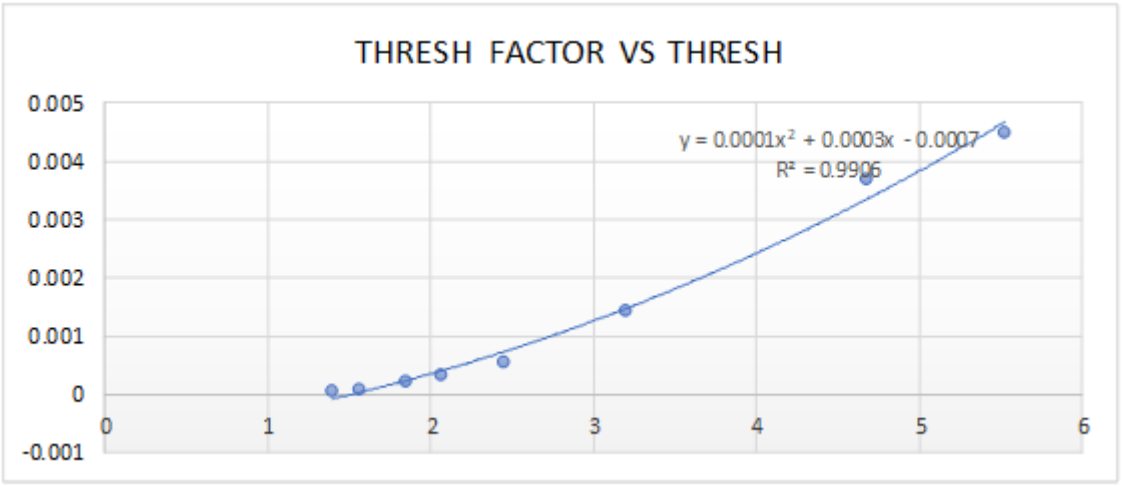

Figure 5: Thresh factor versus thresh value

Figure 6 shows the flow chart used to analyze the image data using a gradient different weight algorithm.

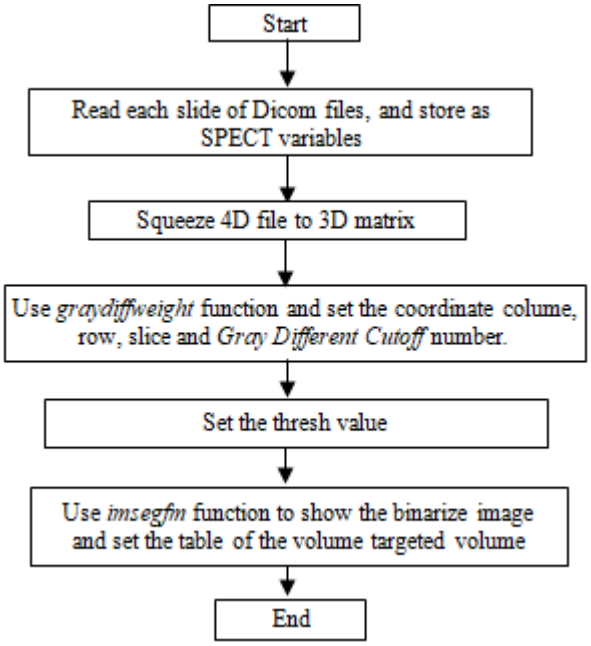

Figure 6: Image processing workflow using gradient different weight method

2.5 Monte Carlo-simulated SPECT images

For validation like real humans, Monte Carlo simulations using the SIMIND program have degenerated using Zubal phantom, as shown in Figure 7. Report number 44 of ICRU provided the densities of several organs. Three tumours were delineated using voxel masks that were originally produced via delineation in patient's SPECT images, as described in [16]. The right and left lungs are each, and another is in the left kidney, as seen in Table 2. Iodine-131 was used as a radiotracer for the lesion. With a medium energy collimator, the simulated camera was able to acquire 64 projections in full rotation mode in 256 x 256 matrices with 4.42mm x 4.42mm pixels. All SPECT images were reconstructed using ordered subsets expectation maximization (OSEM) using an offline programme.

Table 2: Lesion on SPECT Monte Carlo simulated

No. of Lesion	Location	Shape	Actual Volume (ml)	Actual Activity Concentration (Mbq/ml)
1	Right Lung	Sphere	2.61	15.9
2	Left Lung	Ellipse	12.82	18.7
3	Left Renal	Ellipse	5.79	21.1

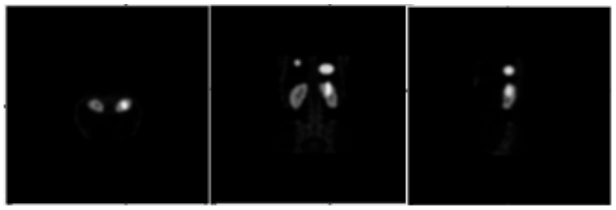

(a)

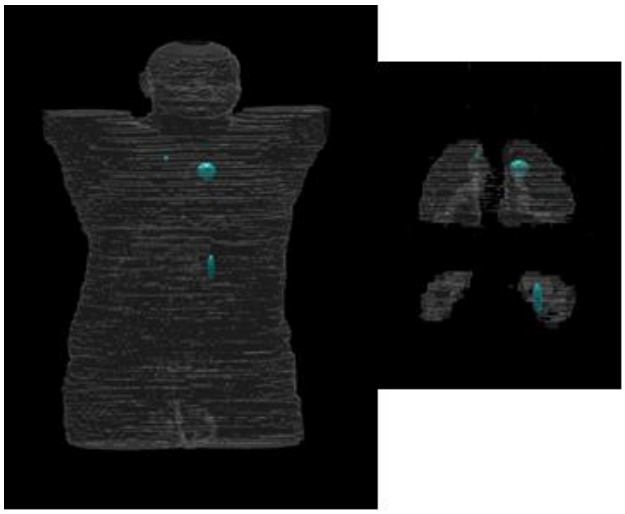

(b)

Figure 7: (a) SPECT imaging simulated with lesion and density organ distribution, (b) 3D Zubal Phantom with lesion inserted

2.6 Evaluation

The results of the method gradient different weight segmentation using the NEMA image and Monte Carlo simulated were evaluated concerning three aspects: volume error, dice similarity coefficient, and activity concentration error.

3. Results And Discuaasions

Based on Figure 5, it can be observed that the thresh factor for background ratio 10:1 and 8:1 has a high regression value (R^2) of 0.9906. However, the displayed trednline thresh factor valid only for the range 0.004478 to 0.00004480. If the thresh factor is larger or less than the range, the volume calculation error will exceed 20%. For validation of the equations obtained in Figure 5, background ratio 12:1 and 8:1 were used to test the accuracy of the plotted equations. Table 3 below shows the data analyzed using a gradient different weight algorithm. The equation $y = 0.0001x^2 + 0.0003x - 0.0007$ was used to obtain the thresh value in the algorithm.

From Figure 8, only four large spheres, namely 26.53 ml, 11.5 ml, 5.58 ml and 2.57 ml, were calculated for the parameters of volume deviation, activity concentration and dice similarity coefficient. In contrast, the other two spheres are not calculated because they are not visible and seem to be the same as the background. All these parameters are calculated using Matlab R2021b software.

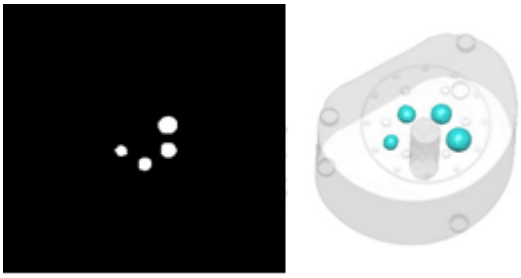

(a) (b)

Figure 8: (a) Image Binarize (b) Three dimensional-3D fusion

The root mean square error (RMSE) for volume computation is 0.42% for background ratio 12: 1 and 0.57% for background ratio 6: 1. Meanwhile, RMSE activity concentration is 0.55% and 0.64% for background ratio 12: 1 and 6: 1, respectively. The dice similarity coefficients respectively show 0.89 and 0.81 for background ratio 12: 1 and 6: 1.

Table 3: Result of NEMA phantom applied gradient different weight method

Method	Background Ratio	Actual Volume (ml)	Volume Calculation (ml)	Deviation (%)	RMSE (%)	Activity Concentration (Mbq/ml)	RMSE (%)	Dice Similarity Coefficient
Gradient Different Weight	12: 1	26.53	26.47	-0.23	0.42	0.271	0.55	0.89
		11.5	11.47	-0.26		0.275		
		5.58	5.5	-1.45		0.279		
		2.57	2.59	0.77		0.277		
		1.15	-	-		-		
		0.52	-	-		-		
	6: 1	26.53	23.31	-0.281	0.57	0.308	0.64	0.81
		11.5	10.86	-0.29		0.289		
		5.58	6.52	-1.42		0.318		
		2.57	2.16	0.81		0.324		
		1.15	-	-		-		
		0.52	-	-		-		

The calculation volumes for the Monte Carlo simulation results were 2.51 ml, 12.37 ml, and 5.67 ml for the first, second, and third lesions, respectively. The first lesion's activity concentration is 14.8 Mbq/ml, 18.1 Mbq/ml and 20.2 Mbq/ml. For dice similarity, Monte Carlo simulated images were not specified.

From the NEMA phantom results obtained, the equation $y = 0.0001x^2 + 0.0003x - 0.0007$ has high accuracy in calculating the volume and activity concentration of the first four spheres in the NEMA phantom. It can be observed that the first sphere has the highest accuracy compared to the other spheres. In this study, the two smallest spheres could not be calculated because the activity concentration sphere is almost the same as the activity concentration background NEMA phantom. To allow the calculation of the two smallest volumes to be made, a high concentration activity such as 20:1 can be performed. For Monte Carlo simulations, even if the targeted volume has an ellipse shape, the calculations can still be calculated accurately. This is because, maximum counts and background counts can be determined accurately.

4. Conclusion And Future Work

The gradient different weight method has a very high accuracy if the background counts can be determined accurately. In addition, it can also be applied to targeted volumes that have various shapes other than spheres.This means that the higher the maximum counts of a targeted volume, the more accurate the calculation of the targeted volume. For the Monte Carlo simulation, the mean background value is easy to determine because we have determined it in the SIMIND code of the program. Even though organs' density differs from the water utilized as a background in the NEMA phantom, there is no substantial difference in the equation $y = 0.0001x^2 + 0.0003x - 0.0007$

when employed in a density apart from water. Future studies will examine the accuracy of volume calculation using the gradient different weight approach with Tc-99m and Lu-177 radioisotopes. By contrast, Matlab gradient different weight algorithm can be likened to the Phyton algorithm. Additionally, the real patient image data set will be used to determine the targeted volume and then the patient thyroid ablation time-activity curve for the dosimetry calculation method.

5. Acknowledgements

The author would like to thank Nuclear Medicine Department at Institut Kanser Negara (IKN) staff for their help, assistance, and cooperation with the data, as well as the Faculty of Applied Science and Technology at Universiti Tun Hussien Onn Malaysia (UTHM) for granting the permission to conduct this study. This study has been approved by the Medical Research and Ethics Committee (MREC), Ministry of Health Malaysia and the study reference NMRR-20-1239-53306 (IIR). This study also had funded by Kementerian Pendidikan Tinggi Malaysia under FRGS grant (FRGS/1/2019/SKK15/UTHM/02/1). The grant is entitled An Algorithm Framework of High-Accuracy Three-Dimensional SPECT-CT Analysis for Efficient Diagnosis of Cancer via Internal Dosimetry Protocol. This study has no conflict of interest. We want to thank the Director-General of Health Malaysia for his permission to publish this article.

References

[1] Y. Li, H. Cai, G. Shen, F. Pang, P. Dong, and L. Li, "Quantification of radioactivity by planar gamma-camera images, a promoted method of absorbed dose in the thyroid after iodine-131 treatment, " *Sci. Rep.*, vol.8, no.1, 2018, doi: 10.1038/s41598-018-28571-y.

[2] S. Faby *et al.*, "Performance of today's dual energy CT and future multi energy CT in virtual non-contrast imaging and in iodine quantification: A simulation study, " *Med. Phys.*, vol.42, no.7, pp.4349–4366, Jul.2015, doi: 10.1118/1.4922654.

[3] Y. K. Dewaraja *et al.*, "MIRD pamphlet no.23: Quantitative SPECT for patient-specific 3-dimensional dosimetry in internal radionuclide therapy, " *Journal of Nuclear Medicine*, vol.53, no.8. pp.1310–1325, Aug.01, 2012, doi: 10.2967/jnumed.111.100123.

[4] V. Thamilarasi and R. Roselin, "Automatic thresholding for segmentation in chest X-ray images based on green channel using mean and standard deviation, " *Int. J. Innov. Technol. Explor. Eng.*, vol.8, no.8, 2019.

[5] D. T. Long, M. A. King, and M. A. Gennert, "Development Of A 3D Gradient-based Method For Volume Quantitation In SPECT, " Aug.2005, pp.1623–1629, doi: 10.1109/nssmic.1990.693614.

[6] W. Jentzen, L. Freudenberg, E. G. Eising, W. Sonnenschein, J. Knust, and A. Bockisch, "Optimized 124I PET dosimetry protocol for radioiodine therapy of differentiated thyroid cancer, " *J. Nucl. Med.*, vol.49, no.6, pp.1017–1023, 2008, doi: 10.2967/jnumed.107.047159.

[7] H. Yong, J. Huang, X. Hua, and L. Zhang, "Gradient Centralization: A New Optimization Technique for Deep Neural Networks, " in *Lecture Notes in Computer Science (including subseries Lecture Notes in Artificial Intelligence and Lecture Notes in Bioinformatics)*, 2020, vol.12346 LNCS, pp.635–652, doi: 10.1007/978-3-030-58452-8_37.

[8] J. Sui, T. Adali, Q. Yu, J. Chen, and V. D. Calhoun, "A review of multivariate methods for multimodal fusion of brain imaging data, " *Journal of Neuroscience Methods*, vol.204, no.1. pp.68–81, Feb.15, 2012, doi: 10.1016/j. jneumeth.2011.10.031.

[9] T. Zhang, Y. Tian, Z. Wang, and Z. D. Wang, "Adaptive Threshold Image Segmentation Based on Definition Evaluation, " *Dongbei Daxue Xuebao/Journal Northeast. Univ.*, vol.41, no.9, 2020, doi: 10.12068/j. issn.1005-3026.2020.09.003.

[10] C. F. Uribe *et al.*, "Accuracy of 177Lu activity quantification in SPECT imaging: a phantom study, " *EJNMMI Phys.*, 2017, doi: 10.1186/s40658-016-0170-3.

[11] A. Bousse, A. Sidlesky, N. Roth, A. Rashidnasab, K. Thielemans, and B. F. Hutton, "Joint activity/attenuation reconstruction in SPECT using photopeak and scatter sinograms, " 2017, doi: 10.1109/NSSMIC.2016.8069448.

[12] M. Fallahpoor, M. Abbasi, F. Kalantari, A. A. Parach, and A. Sen, "Practical nuclear medicine and utility of phantoms for internal dosimetry: Xcat compared with zubal, " *Radiat. Prot. Dosimetry*, vol.174, no.2, 2017, doi: 10.1093/rpd/ncw115.

[13] T. Nakahara *et al.*, "Use of a digital phantom developed by QIBA for harmonizing SUVs obtained from the state-of-the-art SPECT/CT systems: a multicenter study, " *EJNMMI Res.*, 2017, doi: 10.1186/s13550-017-0300-5.

[14] R. A. Gregory *et al.*, "Standardised quantitative radioiodine SPECT/CT Imaging for multicentre dosimetry trials in molecular radiotherapy, " *Phys. Med. Biol.*, vol.64, no.24, 2019, doi: 10.1088/1361-6560/ab5b6c.

[15] W. Zhao *et al.*, "Determination of gamma camera calibration factors for quantitation of therapeutic radioisotopes, " *EJNMMI Phys.*, vol.5, no.1, 2018, doi: 10.1186/s40658-018-0208-9.

[16] G. Brolin, J. Gustafsson, M. Ljungberg, and K. S. Gleisner, "Pharmacokinetic digital phantoms for accuracy assessment of image-based dosimetry in 177Lu-DOTATATE peptide receptor radionuclide therapy, " *Phys. Med. Biol.*, vol.60, no.15, 2015, doi: 10.1088/0031-9155/60/15/6131.

Author Profile

Mr Mohd Akmal bin Masud is a medical physicist at Nuclear Medicine Department Institut Kanser Negara, Malaysia. He obtained his Bachelor of Science (Health Physics) from the Universiti Teknologi Malaysia in 2009. Mr Mohd Akmal bin Masud is developing his expertise focusing on targeted radionuclide dosimetry, image processing and segmentation imaging in nuclear medicine.